**Atmospheric
Chemistry
and Physics
Discussions**

Liquid water content
and effective number
density

Y. Hu et al.

Global statistics of liquid water content and effective number density of water clouds over ocean derived from combined CALIPSO and MODIS measurements

Y. Hu[1], M. Vaughan[1], C. McClain[2], M. Behrenfeld[3], H. Maring[4], D. Anderson[4], S. Sun-Mack[1], D. Flittner[1], J. Huang[1], B. Wielicki[1], P. Minnis[1], C. Weimer[5], C. Trepte[1], and R. Kuehn[1]

[1]NASA Langley Research Center, Hampton, VA, USA
[2]NASA Goddard Space Flight Center, Greenbelt, MD, USA
[3]Oregon State University, Corvallis, OR, USA
[4]NASA Headquarter, Washington, D.C., USA
[5]Ball Aerospace & Technologies Corp., Builder, CO, USA

Correspondence to: Y. Hu (yongxiang.hu-1@nasa.gov)

Title Page

Abstract	Introduction
Conclusions	References
Tables	Figures

◄◄	►►
◄	►
Back	Close

Full Screen / Esc

Printer-friendly Version

Interactive Discussion

EGU

Abstract

This study presents an empirical relation that links layer integrated depolarization ratios, the extinction coefficients, and effective radii of water clouds, based on Monte Carlo simulations of CALIPSO lidar observations. Combined with cloud effective radius retrieved from MODIS, cloud liquid water content and effective number density of water clouds are estimated from CALIPSO lidar depolarization measurements in this study. Global statistics of the cloud liquid water content and effective number density are presented.

1 Introduction

Water clouds are one of the most understood objects for lidar data analysis, since the single scattering properties follow Mie theory and multiple scattering can be estimated from lidar depolarization measurements using a simple formula found by Hu et al. (2006).

There are differences between water cloud measurements from space-based lidar and passive remote sensing instruments. Passive remote sensing of clouds, which measures spectral differences of reflected sunlight and thermal emissions by water clouds, retrieves optical depths of clouds of the entire vertical column accurately for optical depth as large as 100. It also provides effective radius information using the absorption in the near infrared solar radiation wavelengths. On the other hand, the dual-polarization, time-resolved vertical profiling lidar measurement of water clouds carries information about cloud top microphysics of optical depth 2 or 3, which corresponds to the portion that starts at cloud top and ends at roughly 50 m into water clouds. Unlike reflected sunlight by water clouds that is mostly multiple scattering signal, water cloud multiple scattering and single scattering contributions to CALIPSO lidar measurements are in the same order of magnitude. The multiple scattering contribution can be separated from single backscatter using the depolarization measurements and

Title Page

Abstract | Introduction

Conclusions | References

Tables | Figures

◄◄ | ►►

◄ | ►

Back | Close

Full Screen / Esc

Printer-friendly Version

Interactive Discussion

EGU

is proportional to how many cloud particles is within the lidar footprint. The lidar measurements thus provide the information for retrieving cloud top extinction coefficient, liquid water content and number density.

Hu and Stamnes (1993) suggested that multiple scattering from water clouds can be well characterized by extinction coefficients and effective radii, and are not sensitive to the variances of droplet size distribution. For passive remote sensing of clouds using intensity only measurements, multiple scattering dominates radiative intensity measurements. The width of size distribution does not impact the measurements. Monte Carlo simulations in this study confirm that the insensitivity of multiple scattering to the width of size distribution is also also true for lidar returns.

Monte Carlo simulations also indicate that we may derive both extinction coefficient and effective radius of water clouds from CALIPSO lidar measurements, using layer integrated depolarization ratios and the slope of exponential decay in the water cloud backscatter. This study adopts the effective cloud droplet radius retrieved for the Clouds and te Earth's Radiant Energy System (CERES) Project from the Moderate Resolution Imaging Spectral-radiometer (MODIS) (Minnis et al., 1995, 2006), as it is less unambiguous and carefully validated. Liquid water content and effective droplet number density are estimated using CALIPSO's lidar depolarization ratio and the effective radius derived from the MODIS data.

The purpose of this study includes two aspects:

The first objective is to help establish water clouds as calibration and validation objects for future satellite lidar missions. The global statistics of the water cloud physical properties from this study will be a shooting target for field measurements and ground based water cloud observations. By comparing with those observations, better theory and methodology for satellite lidar data analysis of water clouds can be introduced.

The second objective is to provide the global climate modeling community with an improved global water cloud microphysics climatology that is relevant to understanding ocean-atmosphere fluxes of dimethyl sulfide and the connection with clouds. For a given climate forcing, the climate system may respond to it in many possible ways.

A climate system with a swamp-like surface or a razor thin mixed-layer ocean may respond to the forcing with fast temperature change. A climate system with deep mixed-layer ocean may respond to changes of climate forcing with changes in cloud albedo to re-balance the top-of-atmosphere (TOA) radiative fluxes and changes in hydrological
5 cycle to re-balance the surface. Since Shaw (1983) suggested that the DMS-cloud interaction can be an efficient way for the combined ocean and climate system to respond to external forcing, many studies have been performed in this area (e.g., Charlson et al., 1987; Han et al., 1998). Meanwhile, accurate measurements of biogeochemical processes and cloud microphysics on a reasonable spatial and temporal scale remain
10 scarce. Coupled with modeling studies, the water cloud microphysics climatology from combined CALIPSO, MODIS and possibly PARASOL observations will improve the water cloud microphysics observations needed for climate sensitivity studies.

1.1 A simple and reliable technique for estimating liquid water content and effective droplet number density from CALIPSO

15 Water cloud extinction coefficient is related to the depolarization ratio of layer integrated lidar backscattering measurements of CALIPSO, as shown in Fig. 1 that is based on a simulation using the Monte Carlo code of Hu et al. (2001). Multiple scattering contributions to the backscatter increase as cloud extinction coefficient increases. Since the depolarization of radiance from water clouds is proportional to multiple scatter-
20 ing, the depolarization ratio increases for denser clouds as well. For smaller particles, when contrasted with large particles, both multiple scattering and depolarization ratio increase faster with extinction coefficient, since bigger particles scatter more in the forward direction and thus reducing the chances of backscatter. The width of the Gamma droplet size distribution, γ, has minimal impact on the extinction coefficient – depolar-
25 ization relation.

An interesting empirical relation among the extinction coefficient β, the effective ra-

Full Screen / Esc

Printer-friendly Version

Interactive Discussion

EGU

dius Re and depolarization δ, illustrated in Fig. 2, is

$$\beta(\frac{R_e}{R_{e0}})^{-1/3} = 1 + 135\frac{\delta^2}{(1-\delta)^2}. \tag{1}$$

Here the unit of Re is in μm and β is in km^{-1}. R_{e0}=1 μm. The value of β is derived from CALIPSO water cloud measurements using the exponential decay of water
5   cloud attenuated backscatter γ' with range r within the clouds, $\gamma' = \gamma_0 e^{-2\eta\beta r}$. After deconvolution, the slope of exponential decay of water-cloud attenuated backscatter, $\eta\beta$, can be obtained using 4 range bins underneath peak water cloud lidar returns. Thus the extinction coefficient β can be derived while applying the simple relation between multiple scattering factor η from Hu et al. (2007),

10   $$\eta = (\frac{1-\delta}{1+\delta})^2. \tag{2}$$

In Fig. 3, the scatter plot of the extinction coefficients derived from CALIPSO data against the corresponding CALIPSO depolarization ratio measurements is very similar to the relationship developed from the Monte Carlo simulation results in Fig. 1.

After retrieving the extinction coefficient, we can apply it to Eq. (1) to derive Re from
15   the depolarization ratio measurements. The de-convolution process, which removes the tail of the instrument transient response function, depends on the response function used, introduces errors and may not always be stable. The errors in the extinction coefficient will be magnified when it is used for deriving effective radius using Eq. (1).

Instead of using the above approach of deriving extinction coefficient and effective
20   droplet radius, we adopted the collocated water cloud droplet sizes retrieved from MODIS 3.7 μm data for CERES (Minnis et al., 2006). Figure 5 shows the distributions of the monthly mean Re from the Aqua CERES-MODIS analysis. The number of photons scattered into the forward direction increases with particle size. Thus, the chance of the photon being absorbed at the near-infrared wavelengths before returning
25   back to space increases with size also. As a result, water clouds with larger droplets

4069

EGU

are darker in the near-infrared wavelengths. The effective droplet radius derived from the absorption at $3.7\,\mu$m reflects the averaged size information of the very top part of water clouds, with a vertical penetration depth similar to the CALIPSO lidar signal.

Using the layer integrated depolarization ratios (Fig. 4) of water clouds, together with the coincident Re from CERES-MODIS cloud retrievals, we can derive the extinction coefficients β and liquid water content LWC of the water clouds,

$$\beta = (\tfrac{R_e}{R_{e0}})^{1/3}\{1 + 135\tfrac{\delta^2}{(1-\delta)^2}\},$$
$$LWC \approx \tfrac{2R_e\beta}{3} = \tfrac{0.002R_e}{3}(\tfrac{R_e}{R_{e0}})^{1/3}\{1 + 135\tfrac{\delta^2}{(1-\delta)^2}\}. \tag{3}$$

Here, LWC is given in g/m^3. R_{e0}=1 μm. Figures 6 and 7 show the monthly mean extinction coefficients and liquid water contenst computed from the CALIPSO depolarization and MODIS effective droplet sizes, respectively. The liquid water content values agree with various historical in situ measurements, e.g., the aircraft-based Gerber probe measurements at the South Ocean Cloud Experiment off the western coast of Tasmania by Gerber et al. (2001).

For water clouds with a mono-disperse droplet size distribution, the water cloud particle number density N can be relatively accurately estimated if the extinction coefficient is known,

$$N_{\mathrm{mono}} = \frac{\beta}{2\pi r_e^2}. \tag{4}$$

In order to derive particle number density N of water clouds with various sizes, an assumption has to be made about the shape of the size distributions. Here we assume a generalized gamma distribution (Hu et al., 1993),

$$n(r) = \frac{N}{\Gamma(\gamma)r_m}(\frac{r}{r_m})^{\gamma-1}\exp(-r/r_m). \tag{5}$$

Here r$_m$ is the mode radius of the size distribution, and γ is the parameter representing

EGU

the width of the size distributions (the larger the γ is, the narrower the size distribution). The particle number density and extinction coefficient can be approximately related as,

$$\beta = 2\pi N \overline{r^2} = 2\pi \int n(r)r^2 dr = 2\pi N(\gamma + 1)\gamma r_m^2, \tag{6}$$

$$Re = \int n(r)r^3 dr \bigg/ \int n(r)r^2 dr = (\gamma + 2)r_{m,} \tag{7}$$

$$N = \frac{\beta}{2\pi(\gamma + 1)\gamma r_m^2} = \frac{\beta}{2\pi R_e^2}\frac{(\gamma + 2)^2}{(\gamma + 1)\gamma} = N_e\frac{(\gamma + 2)^2}{(\gamma + 1)\gamma}. \tag{8}$$

The effective number density, $N_e = \frac{\beta}{2\pi R_e^2}$, can be derived from depolarization ratios and Re,

$$N_e = 1000\frac{1 + 135\delta^2/(1 - \delta^2)}{2\pi(\frac{R_e}{R_{e0}})^{5/3}}. \tag{9}$$

Here the number density is expressed in cm^{-3}. R_{e0}=1 μm. Comparing with the true droplet number density N, the effective number density is more relevant to absorption in the near infrared and thus to the cloud albedo. But it is not as closely related to CCN as the true droplet number density.

The difference between N and N_e are probably always less than 50%. And the difference can always be estimated with information about the width of the droplet size distribution. The effective number density N_e is the same as the true number density N for very narrow size distributions and thus large γ values, where $\frac{(\gamma+1)\gamma}{(\gamma+2)^2} \approx 1$. In general, the effective water cloud droplet number density is less than the true number density and the difference increases with the width of the size distribution. Note that the variance divided by the mean square of the gamma distribution is γ^{-1}. Values of $\gamma > 10$ require the variance of the gamma distribution to be less than 0.1. Breon and

Liquid water content and effective number density

Y. Hu et al.

Title Page

Abstract | Introduction

Conclusions | References

Tables | Figures

◀ | ▶

◀ | ▶

Back | Close

Full Screen / Esc

Printer-friendly Version

Interactive Discussion

EGU

Goloub (1998) suggest that the variance of water cloud droplet size distribution can be as small as 0.02, while analyzing the angular pattern of the linear polarization from the POLDER measurements. For water clouds with a 0.1 variance in size distribution, the effective number density N_e is 20% smaller than the true cloud number density. Miles et al. (2000) compiled all the available aircraft in situ measurements of water clouds and found the largest variance is slightly smaller than 0.2, of which the difference between Ne and the true number density can be as big as 40%. Any knowledge of the width will help make that difference smaller. The CERES-MODIS retrievals use a modified gamma distribution having an effective variance of 0.1 (Minnis et al., 1998).

Figure 8 shows the global and seasonal distribution of the water cloud effective number density. The true water cloud droplet number density can be estimated from Eq. (8) using climatological values of size distribution widths. The errors of the number density can be assessed using the size distribution width information retrieved from polarization measurements of the glory scattering angle and rainbow scattering angles.

It may be misleading not to look at cloud fraction at the same time as we study cloud microphysics since it may play an equal or probably more important role in cloud climate feedbacks. Figure 9 shows the probability of low level water cloud presence detected by CALIPSO.

2 Discussion

Using depolarization ratio together with effective radius derived from combined CALIPSO and MODIS measurements, we can derive the effective cloud particle number density of water clouds. When the width of the cloud droplet size distribution is known, the true number density can be accurately estimated from the effective number density. Statistics of the true water cloud particle number density will be compiled in the future, using climatology of size distribution width estimated from rainbow and glory information in PARASOL data, as well as other climatological values of size distributions from ground and in situ measurements.

The spatial and seasonal variations of water cloud effective droplet number density derived from this study show some similarity to ocean biogeochemistry processes. It shows similar patterns of DMS concentration seasonal and temporal variations in the middle and low latitudes, generated from the POP Ocean GCM by Chu et al. (2004). Further similarities are noticed between the seasonal and spatial variations of N_e and the ocean primary productivity and phytoplankton, especially at middle to high latitudes, consistent with the observations of Meskhidze et al. (2006).

Probably as important to the sulfur cycle and cloud microphysics hypotheses suggested by Shaw (1983), the ocean mixed-layer depth change and the corresponding changes in low level water cloud amount may be as efficient in terms of re-establish the balance of TOA and surface radiative fluxes. Both require more studies using combined active and passive remote sensing of the ocean and the atmosphere.

One could also estimate cloud physical depth from the MODIS optical depth/LWP and the retrieved LWC. Furthermore, with CALIPSO and CloudSat together, there is possibility of retrieving N_e since CloudSat will give you physical thickness when the cloud base is higher than 1 km.

References

Breon, F. M. and Goloub, P.: Cloud droplet. effective radius from spaceborne polarization. measurements, Geophys. Res. Lett., 25, 1879–1992, 1998.

Charlson, R. J., Lovelock, J. E., Andreae, M. O., and Warren, S. G.: Oceanic phytoplankton, atmospheric sulfur, cloud albedo and climate, Nature, 326, 655–661, 1987.

Chu, S., Elliott, S., Maltrud, M., et al.: Ecodynamic and Eddy-Admitting Dimethyl Sulfide Simulations in a Global Ocean Biogeochemistry/Circulation Model, Earth Interactions, 8, doi:10.1175/1087-3562, 2004.

Gerber, H., Jensen, J. B., Davis, A. B., Marshak, A., and Wiscombe, W. J.: Spectral Density of Cloud Liquid Water Content at High Frequencies, J. Atmos. Sci., 58, 497–503, 2001.

Han, Q., Rossow, B., Chou, J., and Welch, R.: Global Survey of the Relationships of Cloud

Albedo and Liquid Water Path with Droplet Size Using ISCCP, J. Climate, Vol. 11, 1616–1528, 1998.

Hu, Y. and Stamnes, K.: An accurate parameterization of cloud radiative properties suitable for climate models, J. Climate, Vol. 6, No. 4., 728–742, 1993.

5 Hu, Y., Winker, D., Yang, P., Baum, B., Poole, L., and Vann, L.: Identification of cloud phase from PICASSO-CENA lidar depolarization: A multiple scattering sensitivity study, J. Quant. Spectros. Radiat. Trans., 70, 569–579, 2001.

Hu, Y., Liu, Z., Winker, D., Vaughan, M., Noel, V., Bissonnette, L., Roy, G., and McGill, M.: A simple relation between lidar multiple scattering and depolarization for water clouds, Optics

10 Letters, 31, 1809–1811, 2006.

Miles, N. J., Verlinde, J., and Clothiaux, E. E.: Cloud droplet size distributions in low-level stratiform clouds, J. Atmos. Sci., 57, 295–311, 2000.

Meskhidze, N. and Nenes, A.: Phytoplankton and cloudness in the southern ocean, Science, 314, 1919, 2006.

15 Shaw, G.: Aerosols as climate regulators: a climate-biosphere linkage?, Atmos. Environ., 21, 985–986, 1987.

Minnis, P., Kratz, D. P., Coakley Jr., J. A., King, M. D., Garber, D., Heck, P., Mayor, S., Young, D. F., and Arduini, R.: Cloud Optical Property Retrieval (Subsystem 4.3), in: Clouds and the Earth's Radiant Energy System (CERES) Algorithm Theoretical Basis Document, Volume III:

20 Cloud Analyses and Radiance Inversions (Subsystem 4), NASA RP1376, Vol. 3, edited by: CERES Science Team, 135–176, 1995.

Minnis, P., Geier, E., Wielicki, B., et al.: Overview of CERES cloud properties from VIRS and MODIS, Proc. AMS 12th Conf. Atmos. Radiation, Madison, WI, July 10–14, CD-ROM, J2.3, 2006.

25 Minnis, P., Garber, D. P., Young, D. F., Arduini, R. F., and Takano, Y.: Parameterization of reflectance and effective emittance for satellite remote sensing of cloud properties, J. Atmos. Sci., 55, 3313–3339, 1998.

EGU
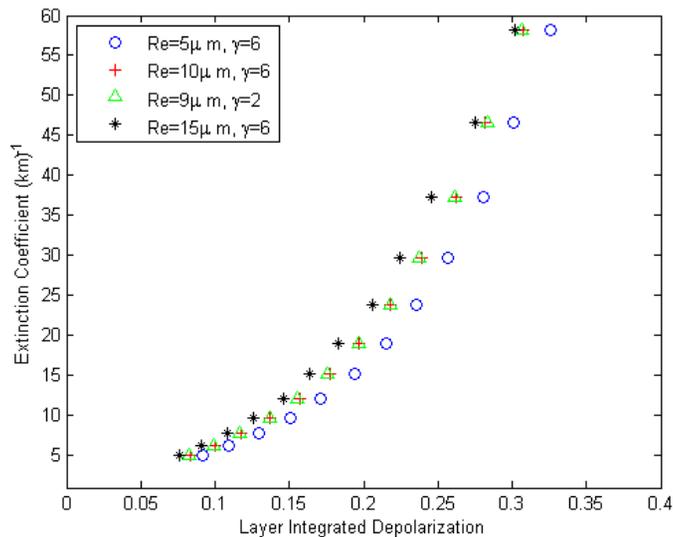
Fig. 1. Theoretical relation between layer averaged extinction coefficients and layer integrated depolarization ratios. Most lidar signal comes from cloud top with optical depth between 0 and 2. The extinction coefficient is thus effectively the average extinction coefficient of within 100 m from cloud top.
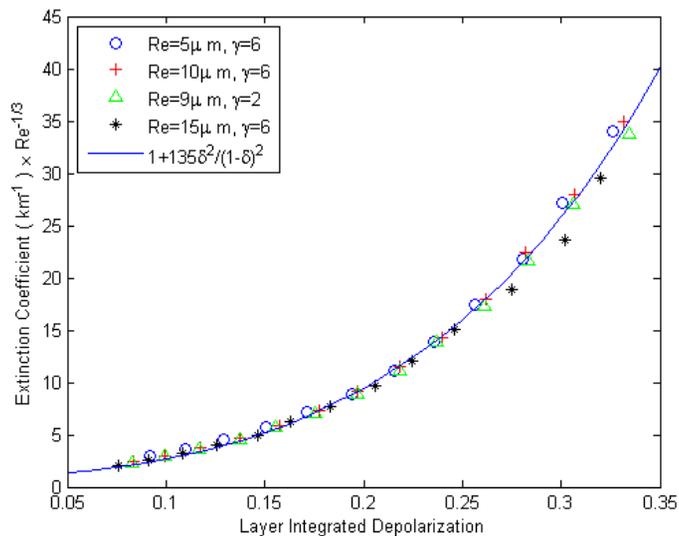
Fig. 2. A simple relation between layer integrated depolarization, extinction coefficient and effective droplet size of water clouds at CALIPSO viewing geometry. This relation is valid for water clouds with different size distributions and extinction coefficients.

EGU
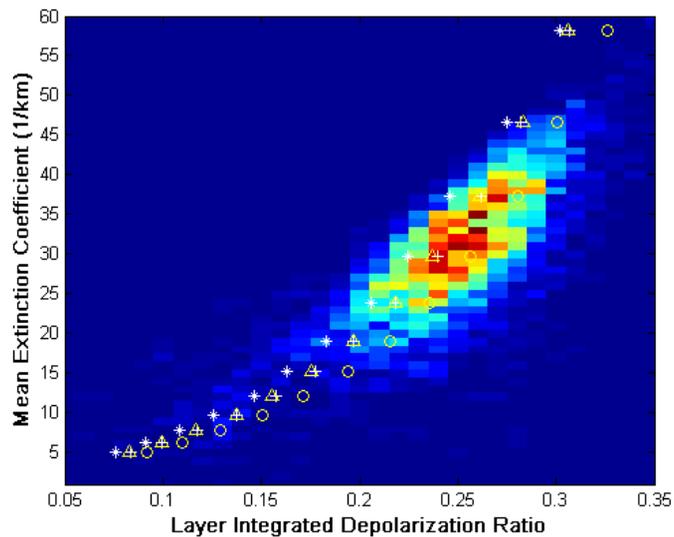
Fig. 3. Histogram of water cloud extinction coefficient and depolarization ratio relation from CALIPSO data. The extinction values are retrieved using CALIPSO vertical profiles. The markers are the modeling results of Fig. 1.

EGU
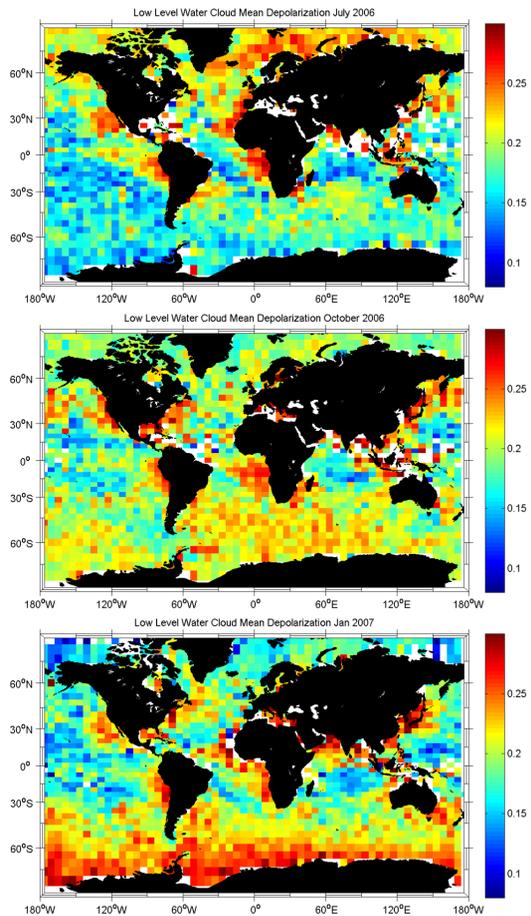
Fig. 4. Monthly mean depolarization of low level water clouds.

Liquid water content and effective number density

Y. Hu et al.

Fig. 5. Monthly mean water cloud effective radii.
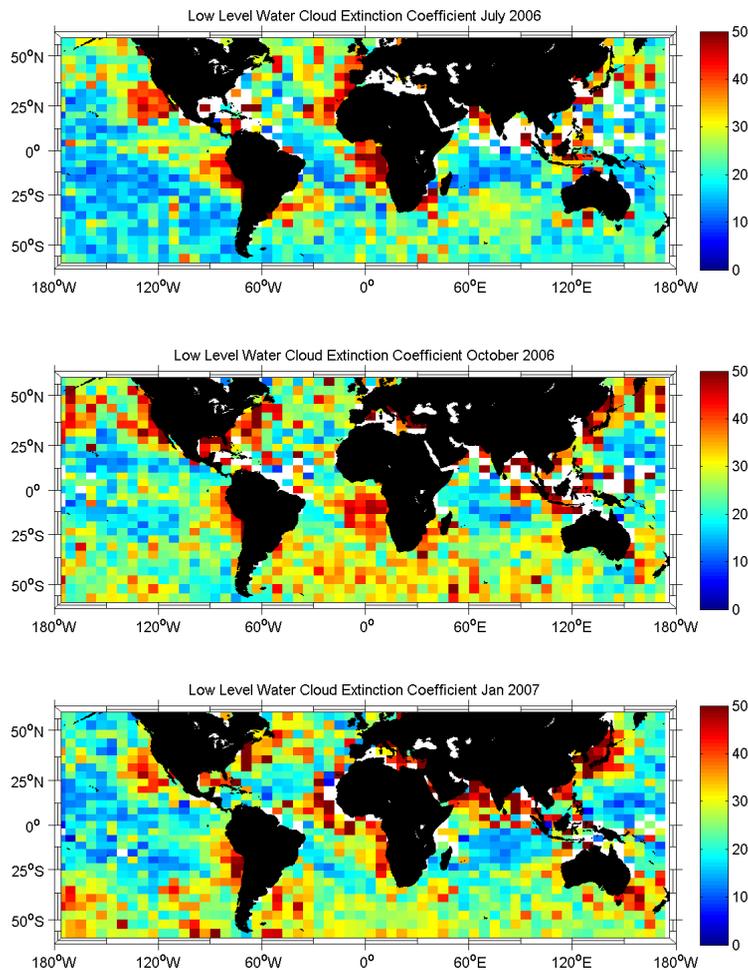
Fig. 6. Monthly mean layer water cloud extinction coefficient (1/km) at various longitude/latitude boxes.

Title Page

Abstract | Introduction

Conclusions | References

Tables | Figures

|◄ | ►|

◄ | ►

Back | Close

Full Screen / Esc

Printer-friendly Version

Interactive Discussion

Fig. 7. Meanly mean Liquid water content of low-level water clouds.

EGU
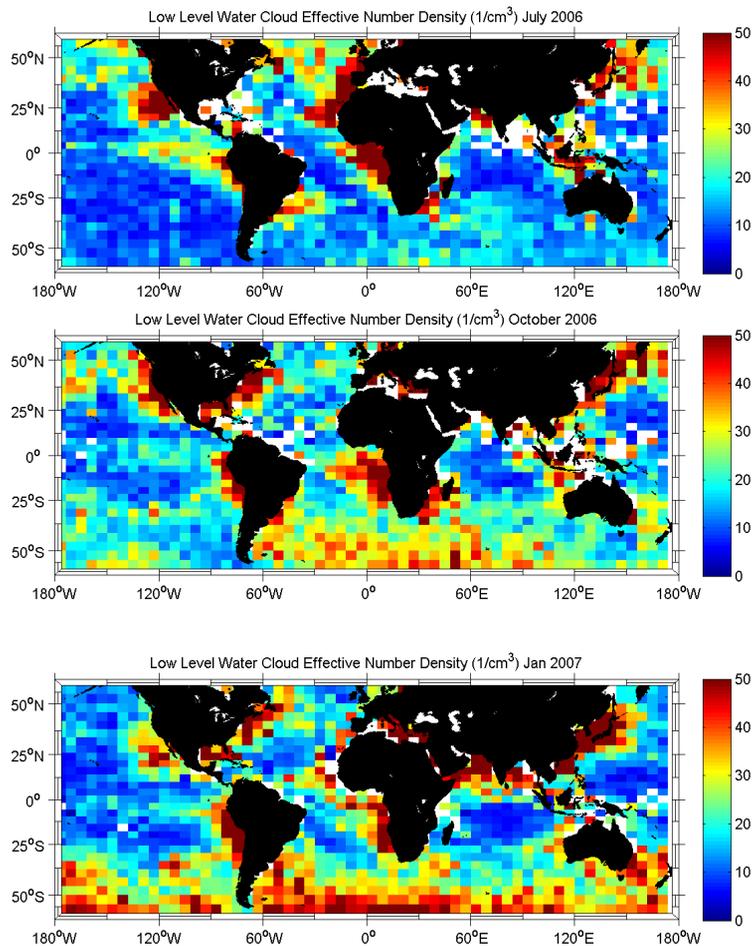
Fig. 8. Monthly mean effective droplet number density of water clouds.

Full Screen / Esc

Printer-friendly Version

Interactive Discussion

EGU
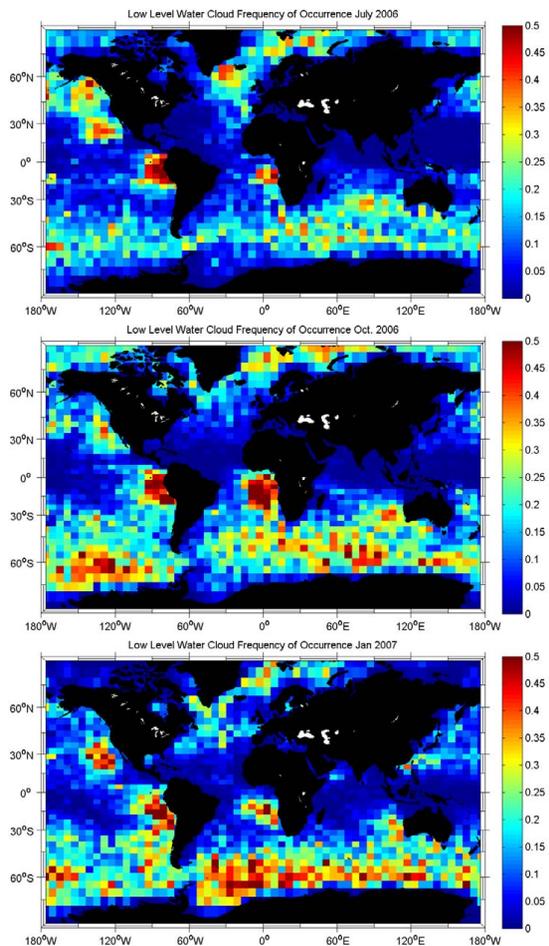
Fig. 9. Frequency of occurrence of water clouds.

EGU